

Design of a Microstrip Bandpass Filter Using Advanced Numerical Models

By Michael A. Imparato, Ryan C. Groulx and Raphael Matarazzo
Aeronix, Inc.

This article describes the design, simulation, construction and performance of a microstrip filter, using advanced analytical component models and TDR-based measurements

Advanced numerical linear circuit models for parallel microstrip coupled line sections have been developed by Applied Wave Research (AWR) for use with their Microwave Office simulation program. The linear elements incorporate closed-form solution techniques that may be evaluated with a linear circuit simulator. The response of the elements provides a high degree of accuracy with respect to electromagnetic simulation, but retain the computation speed of linear simulation. The elements can be used as an alternative to conventional coupled line circuit and electromagnetic models

The linear elements incorporate closed-form solution techniques that may be evaluated with a linear circuit simulator. The response of the elements provides a high degree of accuracy with respect to electromagnetic simulation, but retain the computation speed of linear simulation. The elements can be used as an alternative to conventional coupled line circuit and electromagnetic models

This article describes how the models were used to design a fifth-order hairpin microstrip band pass filter. A yield analysis was performed to verify measured data results. The transmission line characteristic impedance was determined using TDR (time domain reflectometry) techniques, to accurately determine the relative dielectric constant of the substrate material, which is necessary in order to verify measured and simulated data.

Advanced Numerical-Based Elements

Applied Wave Research has developed accurate advanced numerical models for microstrip edge coupled lines, which are labeled MXCLIN elements. "X," which can range from 3 to 16, represents the number of parallel edge-coupled microstrip lines. Figure 1 shows a 4-section edge-coupled line model (M4CLIN). Resistive losses in the metal and dielectric losses in the substrate are characterized in these models [1].

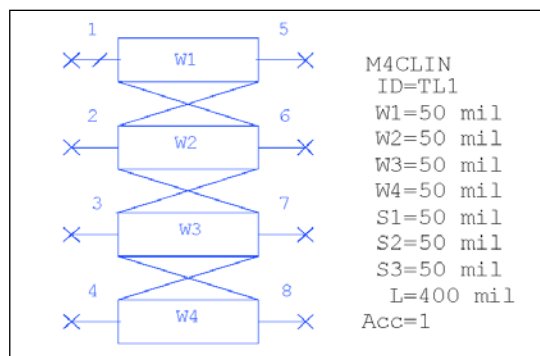


Figure 1 · AWR MXCLIN advanced numerical element model where X = 4.

The advanced numerical models developed by AWR have a user controlled accuracy parameter (Acc). The range of the accuracy parameter can vary from 1 to 10, where 1 is the default value. The accuracy parameter controls the resolution, or mesh, of the computation. If the accuracy parameter is increased, then the density of the mesh will increase, resulting in a greater number of unknowns and increased simulation time.

The accuracy of the advanced numerical models can be attributed to the well-defined closed-form integral expressions that are used to solve for the voltages and currents on the conductors. The advanced numerical models use the integral equation (IE) technique [2] in order to formulate the closed form expressions. Details for the formulation of the models can be found in [3].

Fifth Order Hairpin Bandpass Filter

A practical yet computationally rigorous structure was chosen in order to demonstrate the effectiveness and accuracy of the linear ele-

MICROSTRIP FILTER

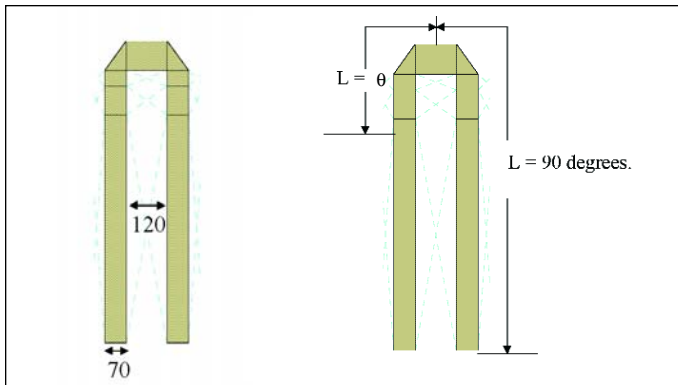


Figure 2 · The single $\lambda/2$ hairpin resonator (left) with the radius and length of the bend chosen for approximately $2W$ spacing between each segment. The resonator tap point location is shown on the right.

ments. The structure under investigation is a fifth-order microstrip band-pass filter with a center frequency of 2.5 GHz. A hairpin topology was chosen so that the MXCLIN elements could be employed. The hairpin topology is a practical approach when real estate is at a premium, however, this configuration is more susceptible to inter-element coupling and radiation effects than a typical straight-line edge-coupled band-pass filter. These effects are accounted for within AWR's MXCLIN elements.

Rogers 4350B dielectric material was chosen as the substrate for this filter. This material was specified to be 30 mils thick with one-half ounce electrodeposited copper.

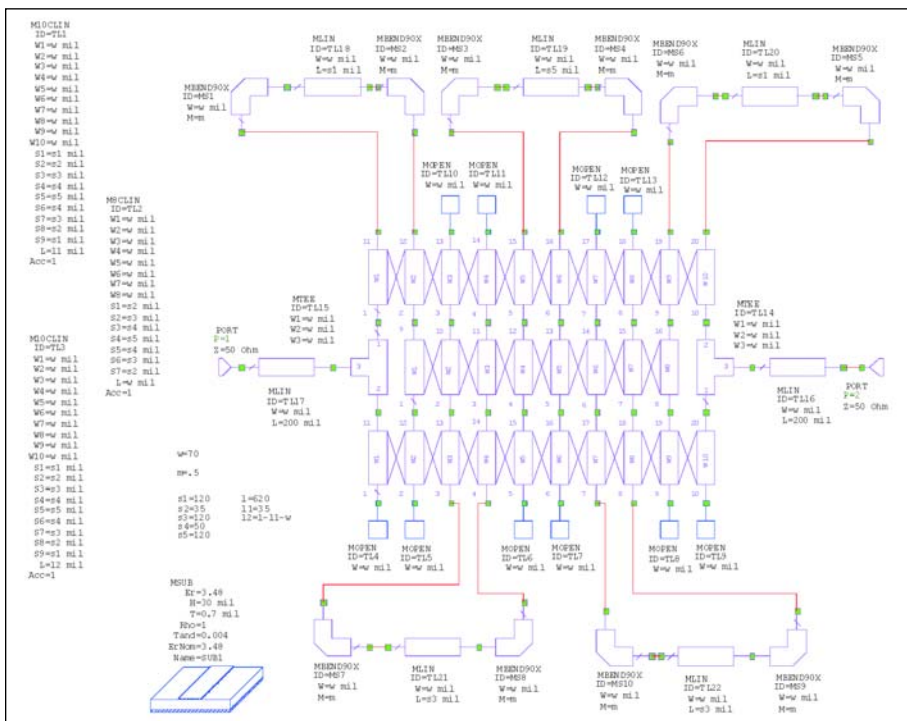


Figure 3 · Microwave Office schematic for the hairpin microstrip filter.

The relative dielectric constant is 3.48 ± 0.05 , and the loss tangent is 0.004. The width of a single microstrip line with an impedance of 50 ohms is calculated to be 68 mils in AWR's TXLINE program. For this analysis, 70 mils was used as the width for all of the lines, as will be described later in this article. The actual impedance of a 70-mil wide line on this material is 49 ohms, as calculated in TXLINE. The mismatch resulting from the use of a 49 ohm line in a 50 ohm system equates to a VSWR of 1.02:1, or a return loss of approximately 40 dB. For all practical purposes, a return loss of 40 dB can be considered a perfect match.

The filter was realized by using tapped inputs and $\lambda/2$ resonators. Each resonator has an electrical length of 180 degrees at the center frequency of 2.5 GHz. Fringing effects of the conductors were taken into account, by using MOPENX elements. The radius and length of the hairpin bend in each resonator was chosen to provide approximately $2W$ spacing between each segment, where W is the conductor width (see Figure 2). The $2W$ design guideline [4] was utilized to minimize inter-element coupling. In addition, a 0.5 mitring fraction for the 90-degree bends was chosen in order to minimize radiation effects at the bends. The location of the tapped input point was chosen to be at the point on the outer resonators that provided the optimum best return loss [5].

Linear and Electromagnetic Models

1. Linear Schematic Model

The linear simulation schematic with advanced numerical models is presented in Figure 3.

The filter schematic was created by using two M10CLIN elements, one M8CLIN element, two MTEE elements, ten MBEND90x elements, seven MLIN elements, and ten MOPEN elements. The M10CLIN and M8CLIN elements incorporate the advanced numerical algorithms, as discussed in the first section of this article.

In the schematic, the M8CLIN element forms the middle section of the filter, and the two M10CLIN elements form the top and bottom sections. The length of the M8CLIN element is set equal to 70 mils in order to compensate for the width of the tapped input and output lines. The tapped lines are implemented by using microstrip T-junction elements MTEEX and transmission line elements (MLIN). The MLIN element is connected to port three of the MTEE element, and ports

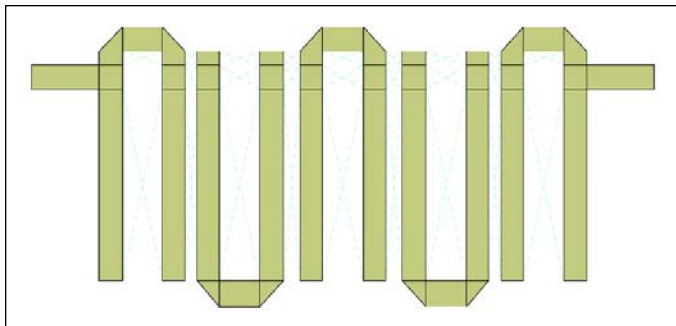


Figure 4 · Filter layout diagram.

1 and 2 are connected to the first line segments of the M10CLIN elements

The hairpin bends are realized by using the MBEND90x elements and MLIN elements. The MBEND90x forms the corner, and the MLIN forms the spacing between opposite ends of a single resonator. In addition, MOPEN elements are placed at each end of the half-wavelength resonators. The MOPEN elements account for the fringing electric field at each of the conductors.

2. Electromagnetic Model

The first step in creating an EM structure is to specify the enclosure parameters. The box dimensions (X and Y) must be defined along with the X and Y divisions. This results in a “cell size.” In this analysis, the X direction was specified to be 1,870 mils (the total length of the filter), and the Y direction 1,500 mils (about 2 times the total width of the filter). The X and Y divisions were specified to be 374 and 300 respectively. This produced a cell size of 10 mils in the X direction and 5 mils in the Y direction. As mentioned earlier, the line widths had to be rounded up from 68 mils to 70 mils to accommodate a 10-mil by 5-mil grid. The physical length of a 180-degree long 50-ohm line is 1,418 mils. Five mils is equal to 0.2% of a wavelength on this material at 2.5 GHz. Therefore, under-meshing is not a concern. The main concern is that there is enough meshing so that the current distribution along the conductor converges to a stable value [6].

Next, the dielectric layers were specified. The top layer is air, 250 mils thick. The second layer is Rogers 4350, 30 mils thick with a relative dielectric constant of 3.48 and loss tangent of 0.004. Finally, the enclosure top and bottom boundaries were set. The top is specified to be an approximate open and the bottom is a perfect conductor.

Next, the layout was copied and pasted as a new EM structure, as shown in Figure 4. With the grid snap turned off, the structure was then manually aligned with the grid dots in the EM layout. (Once the structure is aligned, the grid snap may be re-enabled.) The entire structure should now be selected and then Snap Shape in

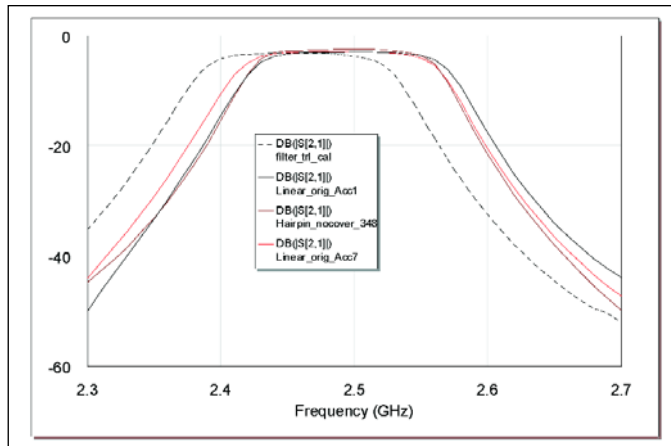


Figure 5 · S_{21} for measured and advanced numerical microstrip elements, with Acc set equal 1 and 7 for the advanced numerical models.

the Draw Menu, should be clicked. This will ensure that the filter is perfectly aligned with the grid and all of the conductors in the filter are evenly divided into 5-mil cells. Finally, the ports are attached to the edge of the structure and de-embedded by shifting the reference plane of the port away from the edge of the box.

Results and Analysis

The microstrip filter board was fabricated using precision photolithography and etching techniques by Protocircuits of Florida, Inc. An etching tolerance of ± 0.7 mils/edge was verified through measurement procedures. The filter was assembled with 50 ohm SMA connectors and measured using an Agilent 8720D VNA (Vector Network Analyzer). A TRL calibration was used for de-embedding the filter’s S parameters from the measurement system.

The frequency sweep for the linear simulation of the advanced numerical models was performed from 2.3 to 2.7 GHz in 0.001 GHz steps. The linear simulations were performed using a Pentium 333 MHz Celeron processor with 256 MB RAM. The accuracy parameter of the model in Figure 3 was varied in order to observe the difference between an increased accuracy parameter setting and simulation time. The transmission coefficient (S_{21}) measured and simulated data are shown in Figure 5. The Linear_orig_Acc1 and Linear_orig_Acc7 curves are the transmission coefficient responses of the simulation with the models Acc parameter set to 1 and 7, respectively. The curve labeled Hairpin_nocover_348 is the response of the Emsight simulation. The curve labeled filtertrl_cal is the measured filter response.

The response of the Emsight simulation matches the response of the Linear_Acc7 simulation on the upper passband frequency skirt, but its response matches the

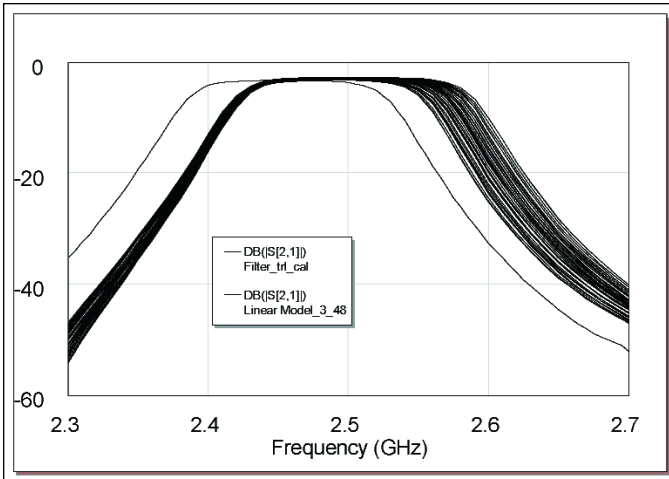


Figure 6 · Yield analysis for the hairpin filter, which considered etching tolerance, substrate thickness tolerance and dielectric constant variation.

Linear_Acc1 simulation on the lower passband frequency skirt. The fact that the Emsight simulation has a slightly narrower bandwidth could be due to the way that Emsight and the advanced numerical models treat the inter-element coupling of the structure.

The Emsight, Linear_Acc1, and Linear_Acc7 constitute the simulated data. The center frequency for all the simulated data is approximately 1.8% higher than the measured data. This is a very significant difference, which was investigated by performing a yield analysis for the specified manufacturing and fabrication tolerances.

The yield analysis was performed by setting the lower and upper bounds of constraint for the specified substrate parameters in the advanced numerical models. An etching factor of ± 1 mil was included by using an equation in the linear schematic to account for the variation in the width and spacing of the coupled line sections. The accuracy parameter (Acc) was set to 1. The dielectric constant was set to 3.48 ± 0.05 for the yield analysis. The conductor

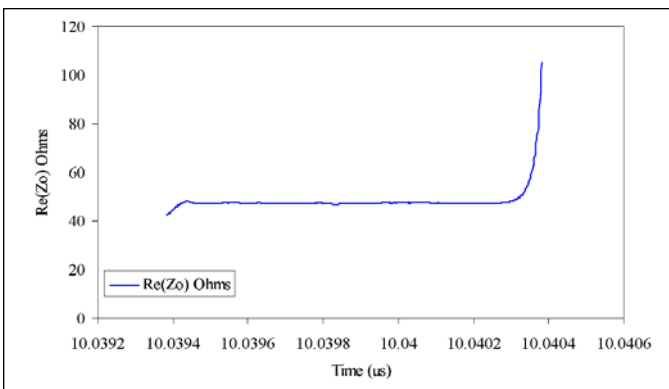


Figure 7 · TDR measurement of the microstrip transmission line for characteristic impedance verification.

width was set to 70 ± 1 mil. The substrate height was set to 30 ± 2 mils.

The result of the analysis, shown in Figure 6, yields a window of variation that is more pronounced on the high end of the filter bandwidth. The upper and lower bounds of the yield analysis results did not encompass the frequency offset between the simulated and measured data. This was anticipated due to the amount of frequency offset and a stated observation from the Rogers 4350B data sheet [7]. The datasheet states that an increase of $+0.2$ in relative dielectric constant (ϵ_r) may be observed in certain cases. Since a higher dielectric constant relates to a lower center frequency, it was determined that the 1.8% frequency offset between the measured and simulated data relates to this $+0.2$ increase in ϵ_r . Therefore, it was necessary to determine an accurate value for the relative dielectric constant of our panel of material.

The relative dielectric constant can be calculated from the effective dielectric constant. The effective dielectric can be obtained through expressions involving the characteristic impedance (Z_0) and the substrate parameters. The effective dielectric can also be obtained by implementing resonator techniques [8] and various relations. In this work, we chose to use Z_0 in order to obtain the necessary parameters.

Characteristic Impedance Measurement

The characteristic impedance of the line was determined using Time Domain Reflectometry (TDR). This involves sending an electrical pulse across a transmission line and measuring the reflected energy. The relationship between the known incident energy and the reflected energy is used to determine the characteristic impedance of the transmission line.

The TDR was performed using the 80E04 TDR sampling module of a Tektronix CSA 8000 Communications Signal Analyzer [9]. The module provides an acquisition rise time of 17.5 ps and a reflected rise time of 35 ps. The averaging acquisition mode of 1,000 samples, and the

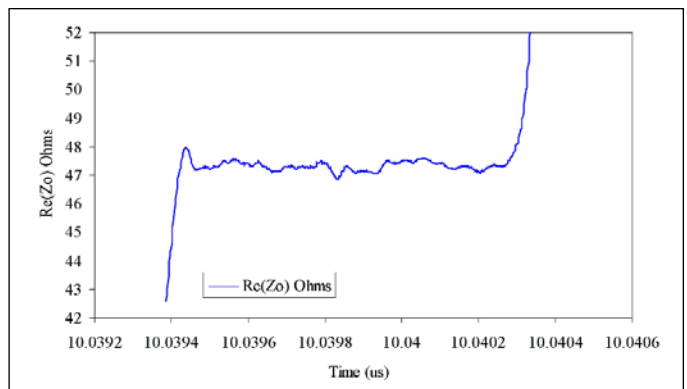


Figure 8 · TDR measurement with the characteristic impedance scaled to 1 ohm per division.



Figure 9 · This measurement window includes the transition from the CSA RF module to the microstrip test board, as well as the coaxial-to-microstrip launch transition from the SMA connector.

maximum resolution of 1 ohm/division were used for the measurement. The CSA 8000 was calibrated by executing the compensation function, which makes the 50 ohm air gap inside the module the reference impedance. With an ideal 50 ohm transmission line, the pulse would travel across the line without any reflections because of a perfect impedance match to the 50 ohm reference.

The microstrip test board was connected directly to the CSA module via a 50 ohm SMA connector. The discontinuity between the module and the test board causes a reflection in the signal path that must be taken into consideration. These reflections are displayed on the analyzer as aberrations such as “ringing” (Figure 9). Observe that the first aberration is caused by the incident TDR pulse that is generated inside the analyzer, and the second aberration is caused by the transition from the module to the test board. The line was terminated as an open circuit, creating another aberration at the end of the line. The characteristic impedance of the line was measured at the steady state value of the response, i.e., beyond the points where the ringing has stabilized. This point is after the SMA launch and before the end of the line (Figure 10).

The TDR was performed on a 3.542-inch delay line fabricated on the same Rogers 4350B panel as the hairpin filter. The delay line is selected to maximize the transition time in order for the pulse to stabilize after it had passed through the discontinuity of the SMA connector. The TDR measurement response is shown in Figures 7 through 10. The measured characteristic impedance had a mean value of 47.31 ohm throughout the line.

Effective and Relative Dielectric Calculations

Once the characteristic impedance was obtained, the

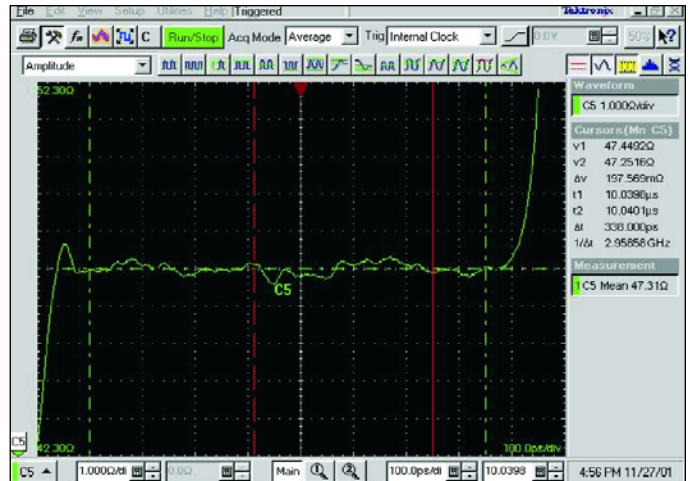


Figure 10 · This measurement window has a narrower scale than Figure 9, showing TDR measurement results for the length of transmission line between the two discontinuities.

effective dielectric was calculated by Equation (1) [2]:

$$\epsilon_{eff} = 1000000h^2 \frac{h^2}{\left\{ Z_{0m}^2 \left[1000W_e + 1393h + 667 \ln \left(4 \times 10^{-3} \frac{250W_e + 361h}{h} \right) h \right]^2 \right\}}$$

Where h is the height of the substrate and η is the free space impedance. We is effective width due to conductor thickness effects, and can be expressed as the following:

$$W_e = \left[\left(\frac{w}{h} \right) + \frac{1.25}{p} \frac{t}{h} \left(1 + \ln \left(\frac{2h}{t} \right) \right) \right] h \quad (2)$$

Where w is the conductor width, t is the conductor thickness. The effective width is valid for:

$$\frac{W_e}{h} > \frac{1}{2p}$$

Since the effective dielectric was obtained from Equation (1), the relative dielectric was obtained from the following equation:

$$\epsilon_{eff} = \frac{\epsilon_r + 1}{2} + \frac{\epsilon_r - 1}{2} \left(1 + 12 \frac{h}{W_e} \right)^{-1/2} - \frac{\epsilon_r - 1}{4.6} \left(\frac{t/h}{\sqrt{w/h}} \right) \quad (3)$$

The characteristic impedance was set to the measured 47.31 ohms. The conductor width was measured and verified to 70.5 mils. The substrate height was measured to be 29.53 mils. The resolution for the height measurement was calibrated to .01 mils. The metal thickness was veri-

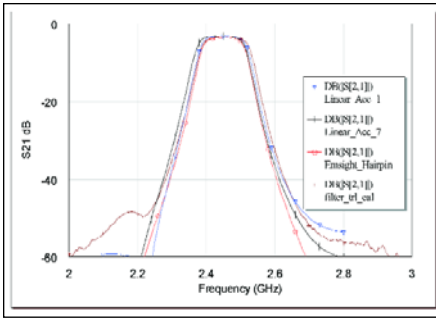


Figure 11 · S_{21} for measured data, advanced numerical models for Acc = 1 and Acc = 7, and Emsight with the calculated parameters from Table 2.

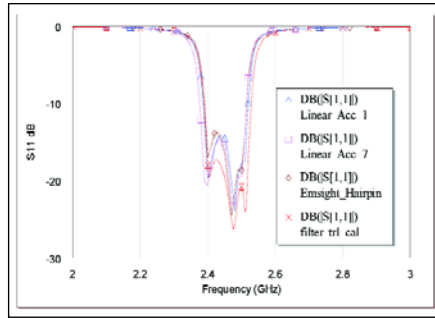


Figure 12 · S_{11} for measured data, advanced numerical models for Acc = 1 and Acc = 7, and Emsight with the calculated parameters from Table 2.

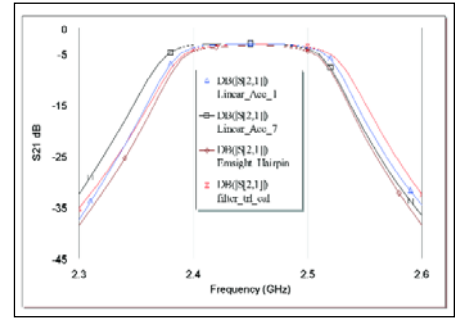


Figure 13 · Narrow band plot of measured data, advanced numerical models (Acc = 1 and Acc = 7) and Emsight with the calculated parameters from Table 2.

fied to be 0.7 mils. The effective and relative dielectric constants were calculated using Equations (1), (2), and (3). The results are summarized in Table 1.

The accuracy of the equations without conductor thickness is better than 0.2 percent [2]. The effect of conductor thickness decreases the relative dielectric constant calculation by .010339, which is .287 percent of the value without considering conductor thickness.

It can be observed that the calculated relative dielectric is 0.13 greater than the nominal specified value of 3.48. This value is within the +0.2 window that is stated in the Rogers 4350B datasheet.

Final Simulations

The calculated values from Table 2 were substituted into the substrate definition for the advanced numerical and electromagnetic models. The transmission and reflection coefficients for the measured data, the advanced numerical model, and the electromagnetic model are shown in Figures 11 and 12, respectively. A narrow band plot for S_{21} is shown in Figure 13. Two curves are labeled Linear_Acc_1 and Linear_Acc_7 for the advanced numerical model response with the accuracy parameter set to 1 and 7. The curve labeled Emsight_hairpin is the electromagnetic model response and the curve labeled filter_trl_cal is the measured response.

Parameter	Value
Z_0 (characteristic impedance)	47.31 ohms
Conductor width (W)	70.50 mils
Substrate height (h)	29.53 mils
Conductor thickness (t)	0.70 mils
Effective dielectric constant (ϵ_{eff})	2.83
Relative dielectric constant (ϵ_r)	3.61

Table 1 · Results for effective and relative dielectric constant calculations.

The electromagnetic model response has a narrower bandwidth compared to the linear models and measured data. This could be due to the differences in modeling the coupling of the structure. The numerical model response bandwidth with Acc set to 1 is 2 MHz narrower than the measured data bandwidth and the numerical model response bandwidth with Acc set to 7 is 2 MHz wider.

The center frequency error of the measured data and predicted data based on the calculated values from Table 2 does not exceed 0.5 percent. The original predicted data and measured data has an error of 1.7 percent. These results agree with the increase in dielectric constant as stated in the Rogers 4350B datasheet.

Conclusion

The design and analysis of a hairpin microstrip bandpass filter was performed by examining AWR's advanced numerical parallel microstrip coupled line models. Accuracy (Acc) settings for the models were investigated and compared with the measured data. A yield analysis was performed in order to verify design results, and it was discovered that the relative dielectric constant of the microstrip line was higher than the expected value.

The possible relative dielectric constant deviation of +0.2 was specified in the Rogers 4350B data sheet. However, in order to verify the measured results of the filter, it was necessary to quantify the actual value of the

Response	Center frequency f_c (GHz)	3 dB bandwidth (MHz)
Filter_trl_cal	2.457	138
Linear_Acc_1	2.452	136
Linear_Acc_7	2.444	140
Emsight_Hairpin	2.450	124

Table 2 · 3 dB bandwidths and center frequency for data in Figure 12.

relative dielectric constant. This was accomplished by performing a TDR characteristic impedance measurement of the microstrip transmission line.

The characteristic impedance was determined to be 47.31 ohms, thus the relative dielectric constant was calculated to be 3.61 with a measured substrate height and conductor width of 29.53 and 70.50 mils, respectively.

The true potential for the advanced numerical models can be realized by accurately characterizing measured results for fabrication and manufacturing tolerances with linear simulation techniques. Varying dimensions by fractional amounts and observing an accurate response may not be feasible with conventional electromagnetic simulations, therefore the advanced numerical models may be used as an alternative to conventional electromagnetic solutions.

Acknowledgements

The authors wish to thank Scott Maynard, Applied Wave Research; Dr. Walter M. Nunn, Jr., Professor, Florida Institute of Technology; Sandii Steele, Technical Sales Manager, Proto Circuits; Mark Roberts, Tektronix, Inc. for use of the CSA8000 for TDR measurements; Sachin N. Dekate, Graduate Student F.I.T.; and Dr. Phil Dipiazza, F.I.T.

References

1. Applied Wave Research, *Micro-wave Office 4.02 On line Reference Manual*.
2. Constantine A. Balanis, *Advanced Engineering Electromagnetics*. John Wiley and Sons, 1989.
3. Miodrag B. Bazdar, Antonije R. Djordjevic, Roger F. Harrington, and Tapan K. Sarkar, "Evaluation of Quasi-Static Matrix Parameters for Multiconductor Transmission Lines using Galerkin's Method," *IEEE Trans. on Microwave Theory and Techniques*, Vol. 42, No.7, July 1994
4. K. Gupta, *Microstrip Lines and Slotlines*, Artech House.
5. Joseph S. Wong, "Microstrip Tapped Filter Design," *IEEE Trans.*, Vol. MTT-27, No. 1, January 1979, pp. 44-50.
6. Warren L. Stutzman, Gary A. Thiele, *Antenna Theory and Design*, John Wiley and Sons, 1981.
7. Rogers 4350B data sheet.
8. R.A. York, and R.C. Compton, "Experimental Evaluation of Existing CAD Models for Microstrip Dispersion," *IEEE Trans.*, Vol. MTT-38, No. 3 March 1990, pp. 327-328.
9. CSA TDR application note.

Author Information

The authors are on the engineering staff at Aeronix, Inc., 1775 W. Hibiscus Blvd., Suite 304, Melbourne, FL 32901. Interested readers may contact Michael Imparato by e-mail at mimparato@aeronix.com